We are IntechOpen, the world's leading publisher of Open Access books Built by scientists, for scientists

4,800
Open access books available

122,000
International authors and editors

135M
Downloads

Our authors are among the

154
Countries delivered to

TOP 1%
most cited scientists

12.2%
Contributors from top 500 universities

CLARIVATE ANALYTICS BOOK CITATION INDEX INDEXED

WEB OF SCIENCE™

Selection of our books indexed in the Book Citation Index in Web of Science™ Core Collection (BKCI)

Interested in publishing with us?
Contact book.department@intechopen.com

Numbers displayed above are based on latest data collected.
For more information visit www.intechopen.com

11

Mesoscopic Modelling of Metallic Interface Evolution Using Cellular Automata Model

Abdelhafed. Taleb and Jean Pierre Badiali
UPMC, Laboratoire d'Electrochimie,
Chimie des Interfaces et Modélisation pour l'Energie
ENSCP, Chimie ParisTech, CNRS/UMR 7575.11 rue P. et M. Curie,
75231 Paris cedex 05
France

1. Introduction

The evolution of metallic surfaces in contact with aggressive environment results from a large number of coupled phenomena operating over wide ranges of time and length scales. Indeed we deal with a large number of chemical species, a combination of many processes (chemical, electrochemical, mechanical ...) and we have to perform a multi-scale analysis both in space and time. To understand and reproduce the rich phenomenology of such systems various approaches are developed from microscopic to mesoscopic and macroscopic levels.

At the atomic scale the main task consists to describe elementary processes involved in a specific metal interface (Arrouvel et al., 1996); (Balazs, 1996); (Balazs, 1995), in this case all the chemical specificities are considered. However the elementary processes are not directly observable but they underlie other phenomena for instance transport phenomena that depend on boundary conditions. This introduces a coupling between microscopic and macroscopic levels of description.

Therefore leaving the microscopic scale some scientists – mainly physicists – have developed an approach in which the main goal (Balazs, 1996); (Balazs & Gouyet, 1995); (Vazquez et al., 1995) is to focus on the general aspects of the processes involved in metal surface evolution. Many processes developed at the level of the interface are considered as irrelevant. This leads to analyse the results in terms of universality classes and scaling laws. These models allow for investigating the morphology of the surface (roughness, dendrites formation, etc …).

Besides these rather recent approaches a huge literature that we call electrochemical to be short, has been developed. It is based on models combining a set of electrochemical and chemical reactions coupled with transport phenomena and an electric potential distribution. These models lead to solve a set of partial differential equations that are purely deterministic.

Hereafter we want to develop an approach that is intermediate between the one developed by physicists and that corresponding to the traditional electrochemical literature. Thus, our main goal is to investigate the evolution of metal surface related to stochastic processes but including realistic electrochemical point of view. However, we do not want to describe a

specific system but rather to analyse how the combination of a small number of basic processes very well accepted by electrochemists might determine general features. Since we do not consider all the processes that may have an important role for a specific system we work at a mesoscopic scale i.e. we assume that a coarse graining is performed on processes at a microscopic scale. Hereafter mesoscopic approaches are considered as a way to combine the macroscopic phenomenology with the stochastic character of the processes originating from the microscopic scale phenomena. The cellular automata (CA) models are particularly suited for describing the physics at a mesoscopic scale. There is also another reason justifying the use of CA models. A large literature concerning the corrosion experiments reveals the stochastic character of some quantities like the incubation time, the corrosion rate, the pit morphology, etc …. Thus using a cellular automata model we have a theoretical tool from which we may expect to reproduce a stochastic behavior.

In parallel, Monte Carlo (MC) simulations (Malki & Baroux, 2005); (Reigada et al., 1994) have been performed, they exhibit some strong similarities with a CA description. An important advantage of CA is that it saves computing time when compared with the MC lattice dynamics where sites are updated randomly in a sequential manner (Kortlük, 1998). CA and MC have found to be in good quantitative agreement for several surface catalytic reactions models once the initial inherent difficulties to an implementation of a parallel procedure has been overcome (Cordoba et al., 2001). However, CA does not seem to have been used extensively in modeling metal electrolyte interface, although this approach has been recognized more efficiency than their MC counterparts (Nishidate et al., 1996), and of course, more suitable for high speed parallel computers.

In recent works we have shown that a cellular automata model is a simple and convenient way to describe interface evolution in contact with aggressive environment taking into account the diffusion (Taleb et al., 2001); (Taleb et al., 2006); (Taleb et al., 2007); (Stafiej et al., 2006); (Vautrin et al., 2007), (Vautrin et al., 2008). A combination of simple processes involving diffusion and chemical reactions represents a typical example of what we want to investigate; this is justified because such phenomena are present in the formation of any oxide layer. The richness of behaviours we observe does not result from the existence of a huge number of processes but from an apparent very simple algorithm. Our main goal is to describe the gross features, which appear in the formation of oxide layers on a metallic surface in the presence of corrosion, precipitation of some reaction products and pH distribution. In particular we will focus on the evolution of the corrosion front and a description of its morphology via its roughness.

The mesoscopic approach is efficient to discover some general tendencies or the coupling between several phenomena. However the weak points of this approach concern the coarse graining procedure that it supposes and the connection with the microscopic scale. In general we are not able to perform this coarse graining explicitly. In some cases it is possible to have a mapping between simulation and experimental results then we may estimate the size of the lattice spacing and to check the consistency of the approach. This has been done in one of our paper (Taleb et al., 2001); (Taleb et al., 2006) in which we have predicted the law of oxide layer growth on a metal surface. This is much more difficult in other cases.

In Section 2 we will develop the main ingredients that are necessary to develop a cellular automata model in general. This implies to define what we mean by the mesoscopic scale, and to give the general conditions needed to realize a CA approach. In Section 3 we describe some simulation results in the case of a planar interface. We will start from the simplest model in which there is no diffusion, this model is equivalent to a double Eden model. Then

we introduce the diffusion of corrosion product and also the Pilling Bedworth coefficient, the feedback effect of the layer in formation on the corrosion rate will be analyzed via several quantities like the evolution of the front, the distribution of walkers and the surface roughness. In Section 4 we improve the previous models by introducing more explicitly some basic chemical and electrochemical processes. This will be illustrated by considering a heterogeneous process in which a metal recovered by an insulating film is put in contact with an aggressive medium due to a local rupture in the film. In Section 5 we present the conclusions and give some perspectives.

2. The main ingredients in a cellular automata description

In this Section we develop the main ingredients that are involved in the cellular automata model.

2.1 The mesoscopic scale

Today the mesoscopic scale is largely developed in the domain of chemical physics associated with the so-called the soft matter physics (De Gennes, 1991). Mesoscopic scale results from a coarse graining procedure which is rarely performed explicitly.

To elaborate a mesoscopic description we are inspired by two archetypal examples in which the coarse graining is performed more or less explicitly. The first one is the Brownian motion (Le Bellac, 1988). To investigate the motion of an ion in a solution we may forget the detailed dynamics associated with the solvent molecules provided the ion mass is much larger than the one of a solvent molecule. Then focusing on the ionic dynamics the solvent gives rise to the sum of a frictional and a random force. In this case the coarse graining (Le Bellac, 1988) can be performed analytically because it is assumed that the ion mass is infinitely large compare to the solvent mass. In our approach, we retain only a given number of processes that are treated explicitly; others generate the stochastic evolution. As in the case of Brownian motion we assume that the neglected processes have a characteristic time much smaller than the ones on which we focus. The second example that we have in mind is the ferromagnetism (Kortlüt, 1988). The spins responsible of the magnetism are localized on the sites of a lattice for which the order of magnitude of the lattice spacing is few angstroms. However if we focus on the long range structure near a critical point for instance we forget the microscopic structure, we replace the spins by larger entities the so called spin block that are localized on a supper lattice for which the lattice spacing is few nanometers. The same idea is used here; instead of all the chemical or electrochemical reactions that take place on the metal sites when we are at a microscopic level we consider that an effective process reminiscent of what happens at a microscopic scale but localized on the sites of a lattice for which the lattice spacing is at a mesoscopic scale. The metal atoms, for instance, are replaced by a given number of metal atoms that behaves as a quasi –particle and the information corresponding to a scale smaller than the lattice spacing are considered as irrelevant.

2.2 Realization of a cellular automata model

In a CA model we represent the system by a discrete lattice and then define its dynamic by rules of transformation of the lattices sites during discrete time steps named simulation time step δt. Our CA model is a combination of several stochastic processes characterized by their

probabilities representing electrochemical and chemical reactions. Depending on the considered corrosion system, the number of species and the local chemistry, the stochastic processes involved will be different.
To perform the simulation we used a two dimensional (2D) lattice. This reduced dimensionality is chosen mostly to save computational time. Certainly, the simulation of a three dimensional system would produce a richer class of behaviors but as we shall see a two dimensional approach is sufficient to describe a lot of processes that are expected to take place in real systems. There is no doubt that a 3D calculation will change the order of magnitude of some quantities but we expect that some phenomena may remain qualitatively the same. On the same footing we may expect that the results quantitatively depend on the geometry of the lattice but that any lattice is sufficient for describing the main features in which we are interested. Here we use a squared lattice (connectivity 4).

2.3 Definition of the lattices sites

For a given interface we define a certain number of species. As mentioned above in the case of metal, we do not consider particles but quasi-particles. The species are quasi-particles that move or are transformed as well defined entities. The state of each lattice site is determined by the dominating species at this point. Some of them are common to all corrosion systems. Usually the lattice sites representing the bulk material are denoted M and we call them metal sites or shortly M sites. Such sites are never in contact with the external aggressive environment by definition. We define two other types of metallic sites, R and P located on the surface of the corroded material and exposed to the aggressive environment. R represents a reactive site, which can be transformed in a passive site P. A P site mimics the presence of a solid entity on the metal surface, which can be dissolved. Other sites may exist but they are related to a specific model as we shall see below.
Each site is referred by two indexes one noted “i” is associated with the column and the other “j” is associated with the position of the row. We assume that the lattice is a cell having N_x columns while the number of rows is not limited; outside this cell we assume periodic boundary conditions.

2.4 Transformation rules of the lattices sites

During one simulation time step, δt, different processes take place. Among the processes associated with different electrochemical or chemical reactions considered some of them correspond to a change in the solid, others take place on the corrosion front but on the liquid side and the last ones appear in the bulk solution. To these different phenomena are associated different time scales. The estimation of these different characteristic times ratio leads to a given ordering in the algorithm associated with the processes. This represents an important part of the model but it is also a quite general problem unavoidable in any theoretical description. For instance, in standard deterministic approaches we have to deal with a series of differential equations each one being characterized by a given time. Then from physical arguments we may compare the characteristic time and select the processes that are relevant for a given time scale. In what follows we assume that the long time is related to the transformation of fresh metal sites M into reactive metal R, δt is the time needed to produce this transformation of the solid. The characteristic time associated with chemical or electrochemical reactions is assumed to be vanishingly small in comparison with δt. On the same way we assume that the interfacial processes producing H^+ or OH^- are very short.

The interfacial properties will be investigated as a function of time $t = N_t\ \delta t$, where N_t is the number of simulation time step. Hereafter δt will be considered as our unit of time and the time will be simply measured by N_t.

2.5 Diffusion process

As mentioned in the introduction the diffusion is a basic process in the formation of oxide layers. Hereafter the diffusion will be described by a random walk process. Since the concentration of the diffusion species may be very high in the neighbourhood of the metal surface we will introduce a steric interaction assuming that at most one diffusing species can occupy a given site. This kind of modeling of the steric interaction is commonly used in the literature (Nicolis et al., 2001) and is referred to as the simple exclusion rule. In order to characterize the diffusion we have to decide how many diffusion steps can be performed during δt. We assume that an elementary diffusion step takes a time $\delta t/N_{diff}$ or that N_{diff} diffusion can be performed during δt. During each time interval $\delta t/N_{diff}$ all walkers noted D attempt to execute one step. Among the four nearest neighbors of a given walker, one is selected at random. If this nearest neighbor is a metal site (M, R), no move is made. If the selected nearest neighbor is a P site free of D species, then the walker is moved to it. The walker stays at its initial position when the selected nearest neighbor is already occupied by a D species. In the simulations the list of walkers (D) is permuted randomly at each time step to avoid spurious correlations with the initial setting of the list.

3. Results on planar interfaces.

To mimic the formation of a layer on a metal surface we consider three main processes: corrosion, diffusion and precipitation. Since these phenomena take place in two different regions of the interface we have to deal with a film which is developing with two fronts: one for the growth and the other one for the corrosion. This leads to investigate the coupling between the two fronts; of course the diffusion will play an important role in this coupling.
In this section we first consider a basic model in which there is no diffusion and then we introduce the diffusion and the Pilling Bedworth coefficient which combines with steric hindrance may produce a layer feedback effect on the corrosion rate.

3.1 A basic model

In Section 2.3 we have defined two kinds of metal sites; those in contact with the aggressive medium noted R and the others corresponding to the bulk metal and noted M. We assume that in contact with the aggressive medium the reactive site R can be transformed into a species P. Thus all the chemical transformations that appears at a microscopic scale are replaced by the transformation that is noted

$$E + R \rightarrow P \tag{1}$$

In which E represents a solution site located in the neighbourhood of the reactive site R that is replaced by the reaction product P. This P is put at random on a growth site that is a E site in contact with a P site. By this process we generate at random a compact layer of connected P sites.
Formally such a description of corrosion can be considered as the reverse of a growth process described via the Eden model (Eden, 1961). The basic model is in fact similar to a double Eden model. An example of layer resulting from this process is shown in Figure 1a-

b. The black part represents the bulk metal, the grey part the layer already formed and the white part is occupied only by E species. The conditions of the simulation are given in the figure captions. In order to give a quantitative information on the growth and the corrosion front we define their mean position. After N_t simulation steps the mean position of the growth and the corrosion front are given according to

$$\langle h_{growth}(N_t)\rangle = \frac{1}{N_x}\sum_{i=1,N_x} h_{growth}(i) \tag{2}$$

$$\langle h_{corr}(N_t)\rangle = \frac{1}{N_x}\sum_{i=1,N_x} h_{corr}(i) \tag{3}$$

In which $h_{growth}(i)$ and $h_{corr}(i)$ are, respectively, for the column i the highest value of j for which there is an P site and a corrosion site. As expected from a simple mean field approach the profiles are linear function of N_t. This also shows that the size of the cell N_x = 2000 is large enough to produce very well defined average; in other words although we have a random process the average appears as deterministic quantities. In the model considered there is no natural time step. For instance if we decide that during δt we proceed to N_{corr} time we we may predict that

$$\langle h_{corr}(N_t)\rangle = h(0) - \frac{N_t N_{corr}}{N_x} \tag{4}$$

which is in total agreement with the simulation results. From (4) we may define a corrosion rate $k(N_t)$ as

$$k(N_t) = \frac{d}{dN_t}\left[h(0) - \langle h_{corr}(N_t)\rangle\right] = \frac{d}{dN_t}\Delta h_{corr}(N_t) \tag{5}$$

Here, the corrosion rate is constant and we have $k(N_t)=N_{corr}/N_x$. This represents the number of corroded sites counted per unit of the initial area, N_x, and per unit of time. Although the random choice of the reactive sites does not affect the evolution of $<h_{gowth}(N_t)>$ and $<h_{corr}(N_t)>$, it determines the geometrical roughness of the fronts defined according to

$$\sigma_{growth}(N_t) = \left[\frac{1}{N_x}\sum_{i=1,N_x}\left(h_{growth}(i) - \langle h_{growth}(N_t)\rangle\right)^2\right]^{1/2} \tag{6}$$

and

$$\sigma_{corr}(N_t) = \left[\frac{1}{N_x}\sum_{i=1,N_x}\left(h_{corr}(i) - \langle h_{corr}(N_t)\rangle\right)^2\right]^{1/2} \tag{7}$$

for which we observe the scaling law of the Eden model $\sigma_{growth}(N_t) \sim N_t^{1/3}$ and the same for the corrosion front. In parallel it is well known that the front exhibits a fractal dimension d_f=1.5 (Barabasi & Stanley, 1995).

3.2 Introducing diffusion and feedback effect

In the previous model the diffusion plays no role this is equivalent to say that the diffusion is infinitely rapid, the P entity just formed may reach any growth site into the layer in formation. Now we may improve the previous model by assuming that the P site performs a random walk before to reach a growth site. In addition we will take into account that the species P has a volume larger than the R one. We take this into account by assuming that a site occupied by the metal contains a number (Φ +1) of M species. Instead of Eq. scheme (1) the corrosion reaction is now formally represented by the following reaction scheme.

$$E + (\Phi + 1)\, M \rightarrow P + (\Phi)\, D \qquad (8)$$

where D denoted the diffusing species, it arises as an intermediate in the conversion of the M species into the corrosion product. Its role is then to redistribute the excess volume arising from (Φ) M via a diffusion process that we mimic as a random walk with steric interaction between the D species as explained in subsection 2.5. In Eq. (8), Φ is the traditional Pilling-Bedworth coefficient. The Eq. scheme (8) is basically different from Eq. Scheme (1). In Eq. scheme (1) the corrosion process is certain when a R site has been chosen, when we use Eq scheme (8) we decide that the corrosion is possible provided we can introduce Φ sites in the neighbourhood of M taking into account that R and D cannot occupied the same site. This steric hindrance produces a feedback effect of the layer on the corrosion rate; this is equivalent to say that the layer induces a overpotential in the corrosion rate.

For a given time step, δt, we select at random a given number, $N_{corr,}$ of reactive sites that we attempt to transform. If Φ=1, for each selected reactive site, now represented by (Φ +1) M, two D species have to be inserted in the oxide layer. Then we adopt the following rule. The selected reactive site R is transformed to a layer site (P) that takes the place of the R initial site. At the same time step one D species starts executing its random walk in the following way. From among the four nearest neighbors of the transformed site, the D species is moved till it reaches a E site connected with a P site i.e. a growth site then it replaces E and it is transformed in a P site integrated in the layer in formation. Each attempt to corrode is successful because we can always place the D species at the newly created layer site without breaking the simple exclusion rule. Thus, N_{corr} reactive sites are transformed at a time step.

If Φ=2, we have to attempt insertion of two new D species. One of the nearest neighbors of the site to be corroded is selected at random. If it is a free layer site both sites are converted to D sites. In the other case we attempt the random selection for the remaining three and then two nearest neighbor sites. If it turns out with the last one that none of the nearest neighbors is a free layer site, we have decided to adopt the rule that the corrosion is impossible. This seems to us the simplest and most physical of a handful of the possibilities one can consider here to remain consistent with the exclusion rule. Thus, in the case of Φ=2, the outcome of an attempt to perform scheme reaction is not a priori certain and depend on the situation in the immediate vicinity of the site selected for corrosion. We have created a feedback effect of the oxide layer in formation on the reaction rate. In this simple case we mimic a limitation of the corrosion rate by a concentration overpotential well known in electrochemistry (Bard & Faulkner, 1980).

The snapshots corresponding to Φ=1 are given in Figure 2a. In the layer the white point correspond to the D species. We can see immediately that the diffusion reduces the roughness of the growth front as already reported in ref (Taleb et al., 2004). A similar result is obtained experimentally with the anodization of copper in thiourea containing acid

solution (Hasseb et al., 2001). The mean positions of the corrosion front are not modified by the diffusion, and in particular the corrosion rate defined in (5) is unchanged. In contrast the position of the growth front is no more a linear function of N_t as we can see on figure 3a. For largest values of N_t we observe $[<h_{growth}(N_t)>-h(0)] \sim (N_t)^{\alpha}$ where α is very close to 0.5 the usual signature for growth processes determined by diffusion (Cabrera & Mott, 1949). For $\Phi=2$ the snapshot corresponds to the figure 2b. The growth front exhibits the same properties as in the case of $\Phi=1$ (see figure 3a) while the evolution of the corrosion front is modified. The comparison of Figure 2a and 2b corresponding to the same value of $N_t = 9\ 10^4$ shows that the feedback effect has two main consequences: the thickness of the layer is reduced and a smoothing of the corrosion front is observed.

In the case of $\Phi=2$ (Fig 3a), the value of $\Delta h_{corr}(N_t)=125$ is attained at the simulation time $N_t=10^5$, whereas in the case of $\Phi=1$ when the feedback effect is absent the same value is already obtained at $N_t=2\ 10^4$. The corrosion rate is reduced by approximately 1 order of magnitude. For the case of $\Phi=2$, we have continued the simulation up to $N_t=4.8\ 10^5$ time steps when $\Delta h_{corr}(N_t)=310$, and it is approximately 8 time smaller than the value extrapolated for the case of $\Phi=1$. Thus, the doubling of the number of D species created by corrosion cannot compensate for the reduction rate, and the thickness of the layer is much larger in the case of $\Phi=1$ than in the case of $\Phi=2$.

For $\Phi=2$ the corrosion front exhibit a parabolic evolution, except for times $N_t \rightarrow 0$, . As seen in Figure 3a, for the largest values of N_t we have $\Delta h_{corr}(N_t) \tilde{} (N_t)^{\alpha}$ where α is 0.58, and longer simulation show a very slow evolution of α toward 0.5, which is the value obtained by the experiments in a similar situation (Hasseb et al., 2001). Figure 3a shows the crossover between two regimes. At short times, $N_t \rightarrow 0$, the corrosion front is not covered by D species and each attempt to corrode a site is successful as in the case of $\Phi=1$. After a given number of corrosion steps the corrosion front is both covered by D species that block the corrosion and on average, $N_{corr}(N_t)$ becomes smaller than N_{corr}. However, the coverage of reactive sites by blocking D species may change because these D species may diffuse. This diffusion can be thought of as being due to other species moving more freely than the D species itself. We have in mind holes, which are free layer sites dispersed between the sites occupied primarily by D species when the concentration of D species is high. A hole can move as a result of swapping with the neighboring D species when they happen to step into it. At a distance away from the corrosion front the holes start penetrating the layer of D sites blocking the front. In this regime the corrosion rate or $N_{corr}(N_t)$ is determined partially by initial corrosion rate and by the motion of holes in the vicinity of the corrosion front. In the asymptotic regime in which almost all of the reactive sites are covered by D species, the corrosion rate is only determined by the diffusion of holes and square root dependence in time is expected. As we shall see in Figure 2, for $N_t=9.10^4$ we are not yet in the asymptotic regime, and therefore, the coefficient $\alpha=0.58$ corresponding to that in Figure 2a describes a crossover situation.

The figure 3b shows how the front positions depend on the value of N_{corr} in the case $\Phi = 2$. A linear behaviour should suggest that the value of $\Delta h_{corr}(N_t)$ obtained for $N_{corr}=1$ and $N_t = 10^5$ (curve a in Figure 3b) should be the same as the one obtained with $N_{corr}=10$ and $N_t=10^4$ (curve b in Figure 3b). This is clearly not the case; the value obtained for $N_{corr}=10$ is approximately one-half of the value resulting from a linear prediction. Because one-half of the prediction corrosion acts have been effectively performed but 10 walkers are injected into each effective corrosion, we might expect that the total thickness of the layer should be larger when $N_{corr}=10$ than in the case of $N_{corr}=1$. The simulations are not in agreement with

these predictions. Therefore, it seems difficult to predict in a quantitative way the effect of the initial corrosion rate on the behaviour of the system. The intricate coupling between the processes can be illustrated by investigating the distribution of walkers in the layer as a function of N_t.

The walker distribution $n_D(j)$ along the direction perpendicular to the initial layer plane is obtained by counting for each line j of the square lattice the total number of walkers on this line. In Figure 4, for $N_{corr}=10$, we compare $n_D(j)$, for $\Phi=1$ and $\Phi=2$, at two different times corresponding to $N_t=10^4$ (Figure 4a) and $9\ 10^4$ (Figure 4b). The walker distributions given in Figure 4b correspond to the snapshots presented in parts a and b of figure 2. The two $n_D(j)$ have the same form; however for $\Phi=1$ the faster advancement of the corrosion front compared to the case of $\Phi=2$ and the slower advancement of the growth front are clearly visible. The part of the distribution located below the maximum corresponds to the corrosion front and we see that $n_D(j)$ tends to be larger when Φ is increased.

The area under the distribution $n_D(j)$ shows that the total number of walkers is strongly reduced by the feedback effect when we go from $\Phi=1$ to $\Phi=2$; however, the gradient of the walker concentration is higher in the later case. Accordingly, the diffusion process is more efficient in the case of $\Phi=2$. Thus, we see that the structure of the diffusion efficiency. The stronger the blocking is, the smaller the number of diffusing species is and accordingly the larger the efficiency of the diffusion is that tends to move away the blocking D species. This illustrates how the simple algorithm that we use leads to a strong competition between processes and finally to results that are difficult to predict.

For $\Phi=1$, and $N_{corr}=3$ several results concerning the walker distribution $n_D(j)$ are presented in Figure 5 (Saunier et al., 2005). Whatever the value of Φ, the occurrence of a point where the concentration remains constant during the corrosion process is observed. The results of simulation shown in Figures 5 suggest approximating the walker distribution in the region where $n_D(j)$ is decreasing by a linear dependence. For $\Phi=1$, this is done in Figure 6 in which we have represented two walker distribution referred by 1 and 2. These distributions correspond to two different times $N_{(t1)}$ and $N_{(t2)}$. They intersect at a given position that we choose as the new origin $x'=0$ and where $n_D(j)=n_m$. For the distribution 1 and 2, the position of the growth fronts are noted X_1 and X_2 while Y1 and Y2 represents the positions for which the saturation appears. In the case $\Phi=2$, the results given in Figure 5c show that the trapezoidal form of the walker distribution represented in Figure 6 should be transformed into a triangular one.

For each walker distribution from the geometrical consideration, we have:

$$\frac{n_m}{1} = \frac{X_i}{X_i + Y_i} \tag{9}$$

Where i=1 or 2. Since n_m is fixed from (9) we obtain

$$\frac{dY_i}{dX_i} = \frac{1 - n_m}{n_m} \tag{10}$$

Now, we consider the two distributions simultaneously. In the part of the layer corresponding to $x' > 0$, the net number of particles increases because X_2 is larger than X_1, i.e., the number of walkers also increasing the thickness of the layer by (X_2-X_1). Thus the number of particles injected in this part of the layer is given by.

$$(X_2 - X_1) + \frac{n_m}{2} X_2 - \frac{n_m}{2} X_1 \tag{11}$$

Because of mass conservation, this number must be equal to the number of particles that migrate from the part x'<0. This number depends on the value of Φ and can be readily estimated as follows. For Φ=1, we have

$$(Y_2 - Y_1)\frac{1 - n_m}{2}, \tag{12}$$

While for Φ=2, we have

$$(Y_2 - Y_1)\frac{1 - n_m}{2} + (Y_2 - Y_1)(\phi - 1), \tag{13}$$

Which reduces to Eq. (12) if Φ=1. Thus, we can write the conservation of particles as.

$$(Y_2 - Y_1)(1 + \frac{n_m}{2}) = (Y_2 - Y_1)[\frac{1 - n_m}{2} + (\phi - 1)]. \tag{14}$$

If we take the derivative of this relation relative to X_2, for instance, and use the value of the derivative given in (10) we can get the value of n_m that only depends on Φ. We have immediately n_m =0.25 for Φ=1 and n_m=0.5 for Φ=2. The simulation results are very close to these theoretical predictions since we find n_m=0.28 for Φ=1 and n_m=0.51 for Φ=2. Thus, the previous analysis of the walker distribution predicts quite well the existence of a point where we have a fixed distribution. From simple arguments of symmetry we may expect that this point has to be located near the initial metal/solution plane. The simulations show that the deviations from the position of the initial plane separation are very small taking into account that the thickness of the layer in the saturation regime corresponds to several hundred units of length.

Another quantity characterizing this model is the surface roughness already defined from equations (6) and (7). The results obtained for N_{corr}=10 are given in Figure 7a. We can see that the influence of Φ is very important on σ_{corr}, for Φ = 1 there is no feedback effect and σ_{corr} increases with Δh_{corr} while for Φ = 2 we are in a regime of saturation in which the diffusion is determining and then the corrosion front is smooth and time independent for large values of Δh_{corr} . Now we may analyze σ_{growth} , this quantity is time independent and very small in comparison of what can be predicted with the Eden model, we conclude that the evolution is determined by a diffusion process. In Figure 7b we may see how the smoothing will results from a diffusion process From the left side of the Figure 7b we see that a rough front of Eden type is obtained after 430 simulation steps in the case Φ =1 while on the right side of the Figure 7b we can see the front in the case Φ = 2 and after 4000 simulation time steps. Points A mark the uppermost and points B the lowermost positions of the corrosion front they show that the roughness. In both cases for a hole the probability of arriving at the point A is larger than the probability of reaching point B. Therefore A is more readily corroded as the point B. As a consequence during the front evolution the front tends to move faster at the position of the site A than at the lower site B until the difference in the probability of corrosion between sites becomes insignificant.

The main results obtained in this Section can be summarized as follows. For a system in which the initial corrosion rate is high compared to the diffusion rate, the corrosion products can stay on the corrosion front and block the corrosion mechanism. The blocking of corrosion sites by the corrosion products can be associated with the concentration over-potential, and the feedback effect of the layer on the corrosion rate is similar to a passivation effect. However, the diffusion is not totally impeached because the holes may arrive in the vicinity of the corrosion front. Thus the long-time behaviour of corrosion rate is no longer determined by the initial corrosion rate but by the diffusion process. The simulation shows the transition between these two regimes. The diffusion of holes produces, as a consequence, a smoothing of the corrosion front.

4. Heterogeneous phenomena and localized corrosion

In order to improve the previous model we introduce explicitly some basic chemical and electrochemical processes and a more sophisticated description of the aggressive medium. This will be illustrated by considering a model of localized corrosion. In Subsection 4.1 the model will be presented and the results will be given in 4.2.

4.1 Model for the electrochemical and chemical.

We consider a piece of metal with a flat surface covered by an insulating layer. Due to a mechanical reason for instance we assume that a single punctual damage is performed in this layer putting in contact the metal with the aggressive environment. To be illustrative such environment is an ionic solution containing a given aggressive ion. Depending on the local acidity or basicity the reactions involved in the corrosion processes will be different. We list them below. There is metal anodic dissolution followed by metal cation hydrolysis in acidic or neutral medium.

$$M + H_2O \rightarrow MOH_{aq} + e + H^+ \tag{15}$$

with corrosion products detached from the surface. The reaction (15) exhibits the very well known autocaytalytic effect that is associated with pitting corrosion. Metal anodic oxidation in basic medium, can be written

$$M + OH^- \rightarrow MOH_{solid} + e \tag{16}$$

It leads to the formation of corrosion products MOH_{solid} on the metal surface. They are associated to cathodic reactions which correspond to reduction of the hydrogen ion or water

$$H^+ + e \rightarrow \tfrac{1}{2} H_2 \tag{17}$$

$$H_2O + e \rightarrow \tfrac{1}{2} H_2 + OH^- \tag{18}$$

depending on the acidity of the environment. When the oxidation and reduction are spatially separated, thereafter named SSE reactions, anodic reactions (cathodic reactions) increase the acidity (basicity) of the environment. This leads to the creation of a pH inhomogeneity in the solution. In contrast, when anodic and cathodic reactions occur simultaneously at the same place or at a distance below a certain length scale both electrochemical reactions compensate with no net acidity or basicity change.

$$M + H_2O \rightarrow MOH_{aq} + \tfrac{1}{2} H_2 \quad (19)$$

$$M + H_2O \rightarrow MOH_{solid} + \tfrac{1}{2} H_2 \quad (20)$$

The occurrence of reactions scheme of Eq. (19) and (20) depends also on acidity of the medium. We refer to the above reactions as localized electrochemical reactions (LE reactions). Note that considering the LE reactions or SSE reactions depends on the length scale selected for the modelling. In our previous work (Vautrin et al., 2007); (Vautrin et al., 2008) we have studied the influence of the LE reactions on the corrosion process. The present study is devoted to the effect of prevailing SSE reactions on the corrosion process.
We assume that the presence of aggressive anions that we do not take into account explicitly may induce additional chemical reactions of MOH_{solid} dissolution (Vautrin et al., 2007); (Vautrin et al., 2008)

$$MOH_{solid} \rightarrow MOH_{aq} \quad (21)$$

which occurs especially in acidic medium. In the following we consider MOH_{aq} as an implicit part of the environment solution; it does not appear explicitly in the model. The ions H^+ and OH^- generated in the solution by SSE reactions diffuse and when they encounter neutralisation occurs:

$$H^+ + OH^- \rightarrow H_2O \quad (22)$$

The previous processes are very well accepted in corrosion science; however we may point out some differences with traditional investigations. Hereafter we consider that the corrosion is initiated by an external factor and we do not investigate the processes producing a breakdown in the protective film. Second we assume that the concentration of the aggressive species is not a determining process. Here we analyse the role of diffusion processes on the local pH in solution. This kind of investigation is absent in many works in which it is assumed that the cathodic reaction does not take place inside the cavity but at the external surface of the material.
As it has been shown besides the direct dissolution of the material a detachment of islands occurs in the evolution of the corroding surface. To describe this phenomenon in the context of our lattice model we define the connectivity of the metallic pieces. The connectivity of two sites in our lattice model is defined such that there is a suite of nearest neighbour (nn) sites of the types M, P or R forming a path from one site to another (Chpard & Droz, 1998). Otherwise they are disconnected. The Von Neumann or 4 - connectivity is used except for the front. Two neighboring front sites are connected if they are both von Neumann nearest neighbors or they have an M site as a common von Neumann neighbour. This prevents the surface of a connected M piece from splitting into disconnected pieces. Thus an island in our model is a whole connected piece of metallic sites disconnected from the main corroding block.
In case of spatially separated electrochemical (SSE) reactions, we assume that anodic dissolution of a piece of metal is accompanied by a simultaneous cathodic reaction. The sites of the two reactions belong to the surface of a single connected piece of material.
The electrochemical and chemical reactions given in Eq. schemes (15) – (22) corresponds to description at a microscopic level, now we have to translate such reactions at the

mesoscopic level i.e. in terms of sites. In addition to the sites E we introduce extra solution sites denoted A and C. The site A (C) indicates that the environment at the position occupied by this site is more acidic (basic) than in the original solution E. To a given site we associate the difference in the numbers of acidic and basic sites, $N_{exc}=N_A-N_C$ located in the nearest neighbourhood of the site. Consequently we speak about acidic, neutral and basic environment for $N_{exc}>0$, $N_{exc}=0$ and $N_{exc}<0$, respectively. We mimic the anodic reactions by Eq. schemes (15) and (16) as

$$R \rightarrow A, \quad N_{exc} \geq 0 \tag{23}$$

$$R+C(nn) \rightarrow P+E(nn), \quad N_{exc} < 0 \tag{24}$$

The "(nn)" is put to indicate the nearest neighbor of the considered site. In Eq. scheme (24) the reactive site is changed into a passive site while C is consumed and a new E site appears. Here we adopt the rule that any surface site S, where S=R or S=P, mediates the cathodic processes with an *a priori* equal probability. We represent cathodic reactions by the Eq. schemes (17) and (18) by

$$S+A(nn) \rightarrow S+E(nn), \quad N_{exc} \geq 0 \tag{25}$$

$$S+E(nn) \rightarrow S+C(nn), \quad N_{exc} < 0 \tag{26}$$

We also adopt a simple exclusion rule. If the nearest neighbors of the surface site are neither E nor A it follows that the S site is blocked by nearest neighbors of C type and such an S site cannot mediate the cathodic process. Therefore the *a posteriori* probability of the SSE reaction depends on the blocking of its cathodic part by the presence of C sites. We repeat the selection from among the other S sites until a free site is found, whatever its position provided it is connected to the site on which the anodic reaction takes place, or until the list of connected surface sites is exhausted. If the cathodic reaction is impossible, the spatially separated anodic and cathodic reactions cannot be realized.

The reaction schemes of Eq. (23)-(26) corresponding to SSE reactions are assumed to be realized with a probability $p_{sse}=1$. It can be lower due the blocking of cathodic reaction discussed above. Finally we can mimic the dissolution of MOH_{solid} by Eq. scheme (21) as.

$$P \rightarrow E \tag{27}$$

The probability of this reaction is taken as $p_{PE}=0.25\ N_{exc}$ if $N_{exc} \geq 0$ and $p_{PE}=0$ otherwise. Similarly to Eq. scheme of (24) the Eq. scheme (28) implies that after the dissolution of a P sites some M sites which are in contact with the solution become fresh R site. To account for diffusion C and A sites created in the SSE reactions execute random walk. The target site is selected at random from the nearest neighbours of the walker. If the target site is E the walker is swapped to it. If the walker is C and the target site is occupied by the walker A or vice versa neutralization occurs that mimics the reaction scheme of Eq (22)

$$A + C \rightarrow E + E \tag{28}$$

In any other case the random walk remains in its initial position. We regulate the diffusion rate with respect to the corrosion rate with N_{diff} being an integer parameter indicating the number of steps random walk we perform for each time step of corrosion. We expect that N_{diff} plays an important role in the corrosion evolution as diffusion tends to smooth out the pH inhomogeneities created by SSE reactions.
The above schemes and the values that we use for the set of probabilities are only qualitative and conceived on what is generally known or accepted about corrosion processes in some class of materials. The number of species and the corrosion processes depend on the system considered. The generic features of the corrosion process should not depend, however, on the detailed form of our assumptions.
We may illustrate this procedure like this. Exploring at random the list of surface sites, we find that for the site i the reaction of anodic dissolution followed by metal cation hydrolysis in acidic or neutral medium can be realized. Then the reactive metal site is transformed in MOH_{aq} that disappears instantaneously in the solution and the i is replaced by H^+ that immediately changes the acidity in the interface i.e. the transformation of a site in the neighbourhood of i is now dependent of what happened in i. When all the possibilities of chemical or electrochemical reactions have been explored the diffusion of H^+ or OH^- and their eventual recombination takes place. Only when we restart a new time step we considered the fresh reactive site created during the previous step. The ordering of events considered in the algorithm describes a physical chemistry picture of a given number of metal corroded systems. However, other choice of ordering can be considered for other corroded system. For instance we may introduce a more sophisticated coupling between reactions and diffusion.

4.2 Results

In Figure 8 we present snapshots obtained at N_{diff} = 6000 as function of the time steps. The solution remains locally neutral and the corrosion front is characterized by a uniform roughness with hemispherical shape in the initial stage of the simulation (Fig 8a). We observe the separation of the solution into acidic and basic zones with an intermediate neutral zone after relatively few hundred simulations time steps (Fig 8b-c). The corrosion front is simultaneously separated into smooth and rough surface zone corresponding, respectively to acidic and basic zones in the solution side (Fig 8b-c). The smooth surface zone follows the lattice symmetry and the rough surface zone has an irregular form (Fig 8b-c). We observe the transition from a homogeneous state to an inhomogeneous one concerning the solution and the corrosion front for every N_{diff} is the earlier this transition appears. This suggests that for each N_{diff} value there exist a critical size of the corrosion cavity. Below this critical size the diffusion of A and C species is efficient enough to ensure the neutralization of all of them. Above this critical size the diffusion is too slow for A and C species to neutralize completely. We will discuss this in more detail later. The smooth and rough zones of the corrosion front can be justified as follows. The part of the corrosion front in contact with the basic solution contains P sites as predominant species. P sites cannot be dissolved in the basic medium and can only be used for cathodic reaction. However, for the P sites with totally basic environment the cathodic reactions cannot take place on it. Consequently the corrosion practically stops there. In contrast, the part of the corrosion

front in contact with the acidic solution can undergo the anodic reaction. Because the probability of this reaction p_{sse}=1 is high the metal corrosion is rapidly developed there leading to a smooth front as already shown (Taleb et al., 2004). It is already interesting to notice that the coexistence of two or more regions that may qualify by smooth or rough has been observed in experiment with Al (Balazs, 1996); (Balazs, 1995).
The stochastic character of the phenomena occurring during the corrosion process can be observed in the Fig. 9a-d where we present the snapshots corresponding to a same choice of probabilities, N_{diff}=100 and approximately the same number of time steps. In Figure 9a we observe a deep cavity developing downwards in contrast to the cavities of Figure 9c-d and developing sideways. In figure 9c-d we can observe that the single anodic zone develops the corrosion either to right side or the left side, respectively depending on some initial asymmetry created by the fluctuation. We observe two anodic zones separated by one cathodic zone in Figure 9b. The evolution of this form leads practically to a double cavity and the two cavities develop sharing the same cathodic zone. The coalescence of theses cavities can be expected. Figure 8 and 9 show that a large class of morphology is already obtained and that it is difficult of characterizing the pits geometry in a simple way.

4.2.1 The critical radius

For a given number of corroded sites, $N_{corrded}$, we define an equivalent radius

$$R_{eq} = \left(\frac{2N_{corroded}}{\pi}\right)^{1/2} \tag{29}$$

representing the radius of the semicircle that we would have if the $N_{corroded}$ sites were placed in it. This radius R_{eq} is just a quantitative quantity that allows a comparison of different results corresponding to very different underlying geometries. From our previous results it appears that R_{eq} is a simple quantity that depends linearly on time and can be interpreted in a simple way (Vautrin et al., 2007).
In Figure 10a we present R_{eq} as a function of simulation time steps, N_t, for several values of N_{diff}. In the initial stage of corrosion all the curves coincide and form a straight line characterized by a common universal slope whatever the N_{diff} value. After this initial stage the slope decreases: the smaller N_{diff} the earlier the decrease is obtained. This decrease occurs simultaneously to the appearance of zones in the solution and at the corrosion front. This can be seen by comparing the Figure 10a and 10b. In Figure 10b we present the relative concentration of A sites, n_A, with respect to all the solution sites as a function of the time steps. The A and C sites are created by an SSE reaction as a pair and disappear in pairs in the neutralization reaction. Consequently the number of A sites is equal to that of C sites. We observe that the fraction of A sites is practically negligible until a certain time step where it begins to grow. The time step for which the fraction of A sites grows corresponds to the time step on which the solution stops to be homogeneous and also to time where R_{eq} versus N_t changes its slope (Figure 10a). All these results illustrate the existence of a critical radius, Rc, separating two regimes in the pit growth.
At the beginning of the process we have a stationary regime for which at each time step we start with neutral solution. When R_{eq}>Rc we have a diffusion controlled regime, the diffusion cannot ensure the complete neutralization of A and C sites. As seen in Figure 8 the

A and C sites survive in the solution forming acidic and basic zones in the globally neutral solution. The fraction of A sites is smaller in the case of large N_{diff} because the diffusion and then the neutralization are very efficient.

There is not a unique definition of R_c, hereafter we decide to fit R_{eq} versus N_t according to two straight lines corresponding to the stationary regime or to the diffusion limited regime. We define the critical point by the coordinates (R_c, T_c) of the crossing point between these two straight lines. In figure 11 we show the behaviour of R_c as a function of N_{diff}. We may use a simple model to analyze these results. First, it seems obvious that larger is N_{diff} larger might be the value of R_c. Second, it is clear that R_c must depend on a characteristic length λthat we have to cover by diffusion in order to favour the occurrence of the neutralization via Eq. scheme (28), smaller is λ larger might be R_c. To estimate λ two limiting mechanisms can be considered in which the neutralization takes place near the surface or in the bulk of the cavity. For the first time (N_t) of the simulation, N_{create} represents the number of ions H^+ and OH^- created during this time step and, in the stationary regime, the only H^+ and OH^- ions present in the solution are those produced during the considered simulation time step. The number N_{create} is proportional to r time the value of the effective radius at time t. If the neutralization takes place on the surface, the distance λ is the mean distance between ions on the surface, we have $\lambda \sim R/ N_{create}$ this is just a pure number depending on geometrical factor and we may expect $R_c \sim N_{diff}$. If the neutralization occurs in the bulk solution we may imagine a mechanism in one or two steps: the ions H^+ and OH^- diffuse into the bulk of the solution where they are neutralized or to reach by diffusion the solution bulk where they are uniformly distributed is not sufficient to the occurrence of the neutralization and additional time is needed to their collisions and neutralization. The first process leads to $\lambda \sim R_c$ leading to $R_c \sim N_{diff}^{1/2}$. If λ is determined by the mean distance between H^+ and OH^- when the homogenization is done we have $\lambda \sim (\pi R^2 / N_{create})^{1/2} \sim R^{1/2}$ leading to $R_c \sim (N_{diff} / R_c^{1/2})$ or $R_c \sim N_{diff}^{2/3}$. The simulation results show that a surface neutralization ($R_c \sim N_{diff}$) is excluded but we cannot decided between the two power laws $R_c \sim N_{diff}^{1/2}$ or $R_c \sim N_{diff}^{2/3}$, it is satisfactory to note that for each of these laws the order of magnitude of the prefactor is 1. The linear dependence between R_{eq} and N_t up to R_c suggests that the same power law must relate the critical time T_c and N_{diff}. Indeed we have verified that it is so. Thus the very crude description that we have proposed is certainly a part of simulation result.

At this level it is tempting to analyze the model by trying a mapping between our results and the real world. This task is not easy because our quantitative result is the couple (R_c, T_c) for which we have no experimental result. If our transition time T_c indicates the time after which we observe the growth of a stable regime we cannot associate T_c with the duration of a nucleation phenomena considered in (Ernst & Newman 2002) since the phenomena determining T_c are not taken into account explicitly in (Ernst & Newman 2002). Nevertheless it seems tempting to assume that the transition appears after T_c =1second and that the radius R_c is approximately 1μm. Let assume that the magnitude of the diffusion coefficient D of the species A and C is about 10^{-5} cm^2sec^{-1} as usually in liquid medium. In our simulation the expression of our diffusion coefficient is $D= 4a^2/ \delta t$ in which a is the lattice spacing and δt the duration of an elementary diffusion step. In the approximation $\lambda \sim R_c \sim 1\mu m$ we have $R_c^2 \approx D N_{diff} \delta t$. From figure 10 we choose the case N_{diff} = 6000 for which we get $\delta t \approx (1/6)\ 10^{-6}$ second and a ≈ 10 nanometres. This approximate calculation gives just orders of magnitude

and shows the coherence of our approach provided the chemical and electrochemical reaction have a characteristic time much smaller than 1microsecond. In parallel we deduce that the time for metal restructuring is $6000\delta t \approx 10^{-3}$ second.

4.2.2 Auto catalytic reaction

One of the peculiar and interesting behaviour predicted by the present model is associated with the transition from what we call the stationary regime to diffusion limited regime described in the above section and characterized by the coexistence of rough and smooth zones. The peculiarity of the transition consists in the combination of two processes. First we have seen that the reaction scheme in the equation (15) or (24) is of autocatalytic type; it means that such reaction appears in acidic medium but the result of it is to increase the acidity. Finally it means that when such reaction appears in one place of the surface it favors the appearance of similar reaction in its neighborhood. These spatial correlations of chemical origin, initiate zones with homogeneous properties. Second, if the diffusion of H^+ and OH^- cannot perform a homogenization of the solution during one time step, i. e. after N_{diff} steps, these zones survive and may grow. Of course the distribution of these zones resulting from stochastic processes determines the pit geometry. Note that in the diffusion regime the size of the pit is three orders of magnitude larger than of the initial damage. Thus we can say that our simulations are able to describe the passage from a mesoscopic to a macroscopic scale.

Here we have an example illustrating the fact that the coupling of a surface autocatalytic reaction with a diffusion process may generate a symmetry breaking leading to spatial inhomogeneities at a macroscopic level. Similar phenomena have been extensively investigated by Prigogine and his coworkers (Glansdorff & Prigogine, 1971) and we are in qualitative agreement with their physical predictions. However we cannot describe quantitatively our results from equations used in (Glansdorff & Prigogine, 1971) based on traditional methods of chemical kinetics, so to say on a mean field approach. The stationary regime corresponds to the formation of a small system in which we have strong correlations between the events that take place on nearest neighbor sites. This is clearly outside the scope of a mean field approach. Undoubtedly our description of corrosion processes is realistic, even though only a part of the complicated phenomena is represented in the initiation of a pit and its evolution. But anyway to describe the beginning of a pit formation leads to consider a small volume where strong correlations exist between the reactants. It seems that this is very far from what is done with the theories developed today and accordingly only simulations can give an insight about the beginning of the pit formation.

5. Conclusions and perspectives

Modeling at a mesoscopic scale using cellular automata model appears as an interesting tool to understand general properties of corrosion processes. In this chapter there is two parts; in Section 3 we essentially focus on the diffusion and the feedback effect of the layer on the corrosion rate, in this part no explicit reactions are taking into account. An example of realistic electrochemical and chemical reactions have been introduced in Section 4, there are associated with a pitting corrosion.

The model developed in Section 3 gives a simple description of a phenomenon of passivation. The blocking of corrosion sites by diffusing species can be associated with the

existence of concentration overpotential. For a system in which the initial corrosion rate is high compared to the diffusion rate, the corrosion products can stay on the corrosion front and slower the corrosion mechanism. In addition to an obvious decrease of the corrosion rate, we may also observe a flattening of the corrosion front. Moreover, if we measure the thickness of the layer relative to the initial position then it has been shown that we can find exactly the parabolic law predicted by Mott and Cabrera including the exact value of the prefactor. We show also that the distribution of diffusing species within the growing layer is characterized by two regimes for the growth. Initially the diffusing species are inserted in the layer at constant flux which increase their concentration and after a certain time it may reach a maximum value. The transition from a constant concentration regime results from the steric exclusion between the diffusing species.

Other aspect of corrosion described here is related to the processes that occur within the corroded cavities of pitting (Section 4). Our main difference with standard approaches is related to the fact that we use a stochastic approach in which the shape of the pit (hemisphere or cylinder) is not prescribed. We reproduce different morphologies of pitting corrosion and we observe the existence of a wall pit roughening transition. The simulations allow for a passage from a mesoscopic to a macroscopic scale. The different properties that we have investigated show a transition from a stationary regime to a diffusion limited regime. This transition is characterized by a morphology changing from a semicircular to an elongated shape. This change is accompanied by the appearance of a non uniform distribution in the wall roughness and by the coexistence of zones having different acidity in the solution. The pit surface is divided into two regions, in which anodic surface is smooth and cathodic one is rough, and these two regions are in contact respectively in the solution side with acidic and basic zones. Thus a global description of the surface neglecting these inhomogeneities will give a very poor description of the pitting corrosion.

The transition is characterized by a critical radius R_c depending on the number of diffusion steps N_{diff} during one simulation time step. By a simple analysis we have established several power laws which characterize quite well the critical behaviour observed in the simulation results. This shows that the correlations between different processes involved in our system are well understood. From our analysis, we can say that the neutralization of ions H^+ and OH^- does not take place on the surface of the pit. The pitting is associated with a autocatalytic reaction coupled with a diffusion process; however at the beginning of the pitting it exists strong correlations between the events and a mean field approximation is not able to reproduce the phenomena, probably only numerical simulations can be used to analyze the pit initiation.

In this chapter we focused on a few number of processes but a lot of other processes can be investigated by a cellular automata model. For instance we may investigate the deviations from the Faraday law, the corrosion of the grain boundaries. Another aspect concerns the surface roughness; the definition (7) is restricted to a mechanical description of the roughness but we may also introduce a chemical roughness showing how many reactive site exist on the surface. The relation between the two definitions of the roughness has not been investigated yet. Many other basic phenomena can be investigated as for instance the adsorption of a given inhibitor on the surface. Obviously some three dimensional approaches will be appreciated.

6. Figures

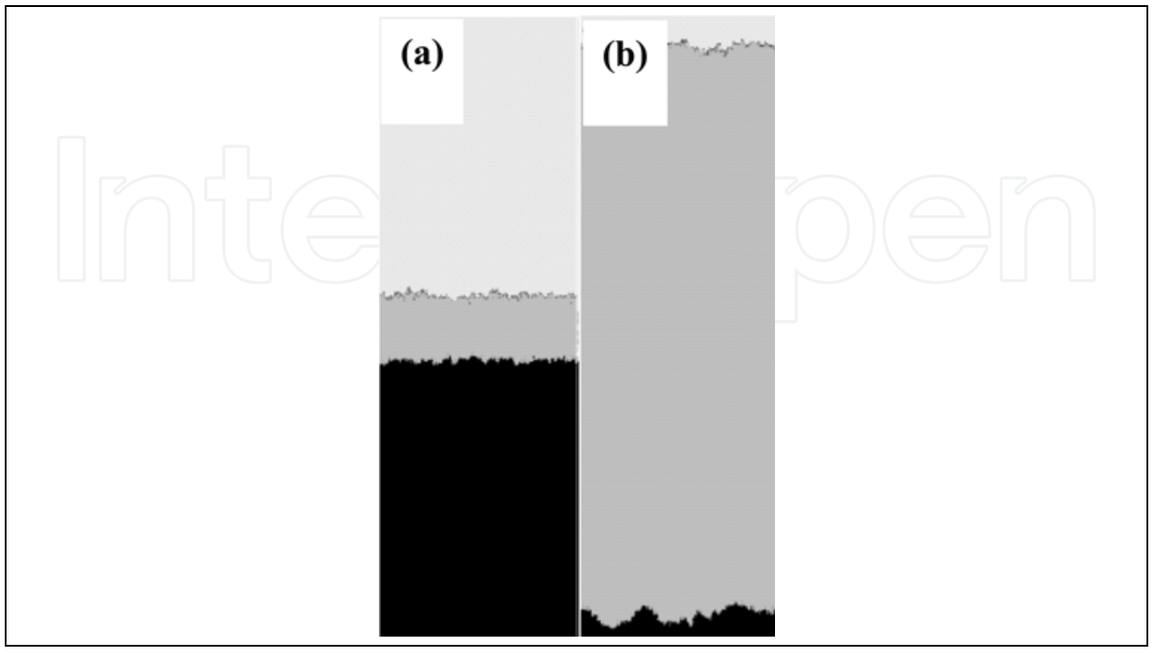

Fig. 1. Snapshots taken at different time step N_t for the double Eden model with N_{corr}=10, N_x = 2000 and (a)- N_t=10000, (b)- N_t=90000.

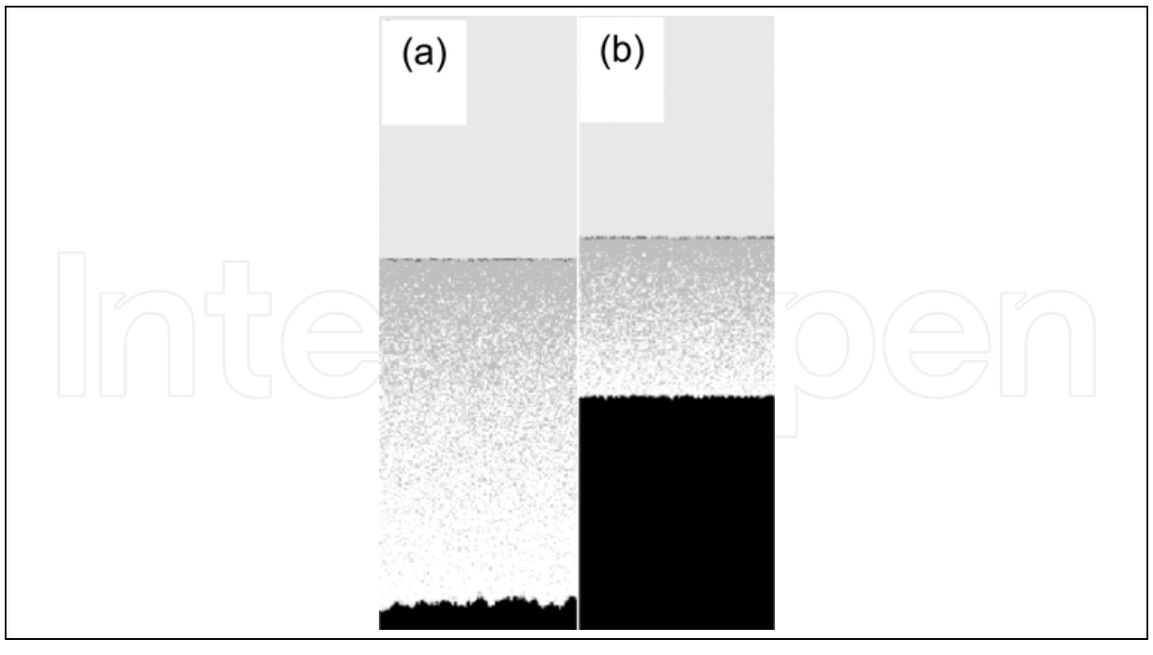

Fig. 2. Snapshots taken at time step N_t =90000, for a- the Eden model for corrosion front and diffusion model for growth with N_{corr}=10 and Φ =1, b- the diffusion model both for corrosion and diffusion front with N_{corr}=10 and Φ =2.

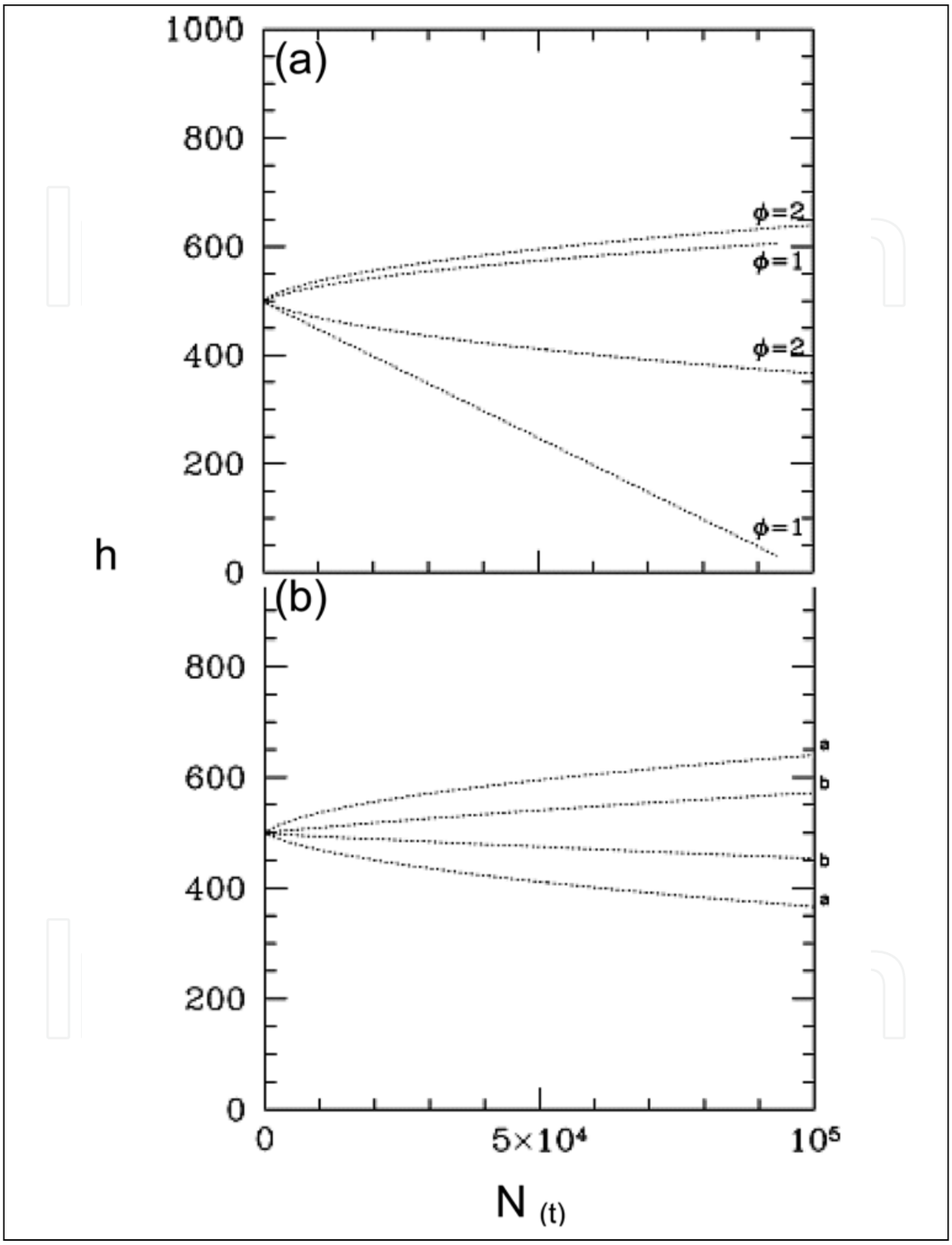

Fig. 3. Comparison of the front evolution in terms of the average positions of the fronts growth (the two upper curves) and corrosion (two lower curves) and for different conditions (a)- N_{corr}=10, Φ=2 and N_{corr}=10, Φ=1; (b)-Φ=2 and a-N_{corr}=10, b- N_{corr}=1.

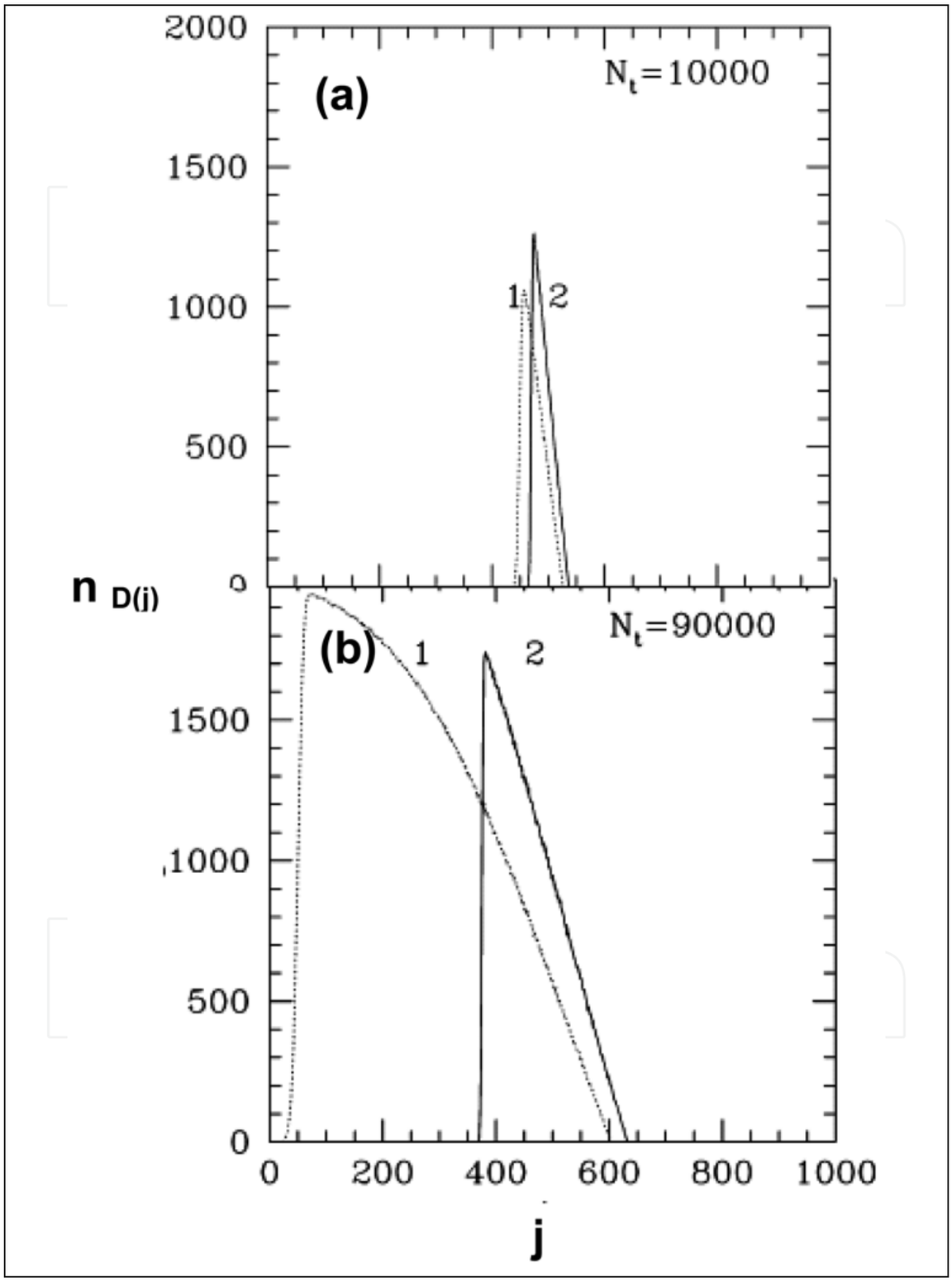

Fig. 4. Distribution of walkers at different simulation time steps (a)- N_t=10000 and (b)- N_t =90000 for the case of Φ =2 (solid line) and Φ =1 (dotted line), N_{corr}=10.

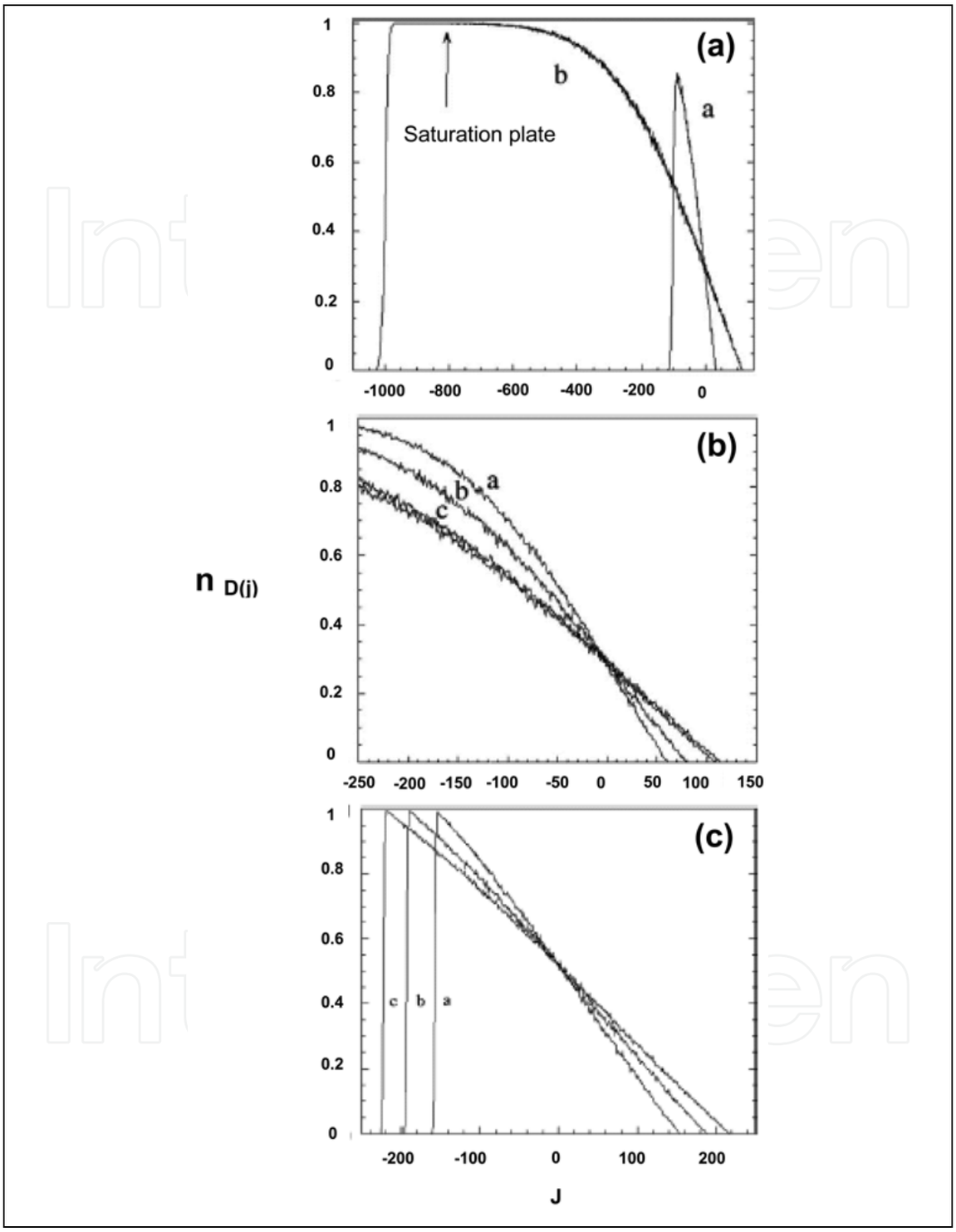

Fig. 5. Walker distribution in the layer obtained for different simulation conditions, (a) N_{corr}=3, Φ=1, N_x=600 and for different times a- $N_t=10^4$ and b- $N_t=10^5$; (b) N_{corr}=3, Φ=1, N_x=600 and for different times a- $N_t=5\ 10^4$, b- $N_t=9\ 10^4$, c- $N_t=10^5$; (c) N_{corr}=150, Φ=2, N_x=600 and for different times a- $N_t=5\ 10^4$, b- $N_t=9\ 10^4$, c- $N_t=10^5$

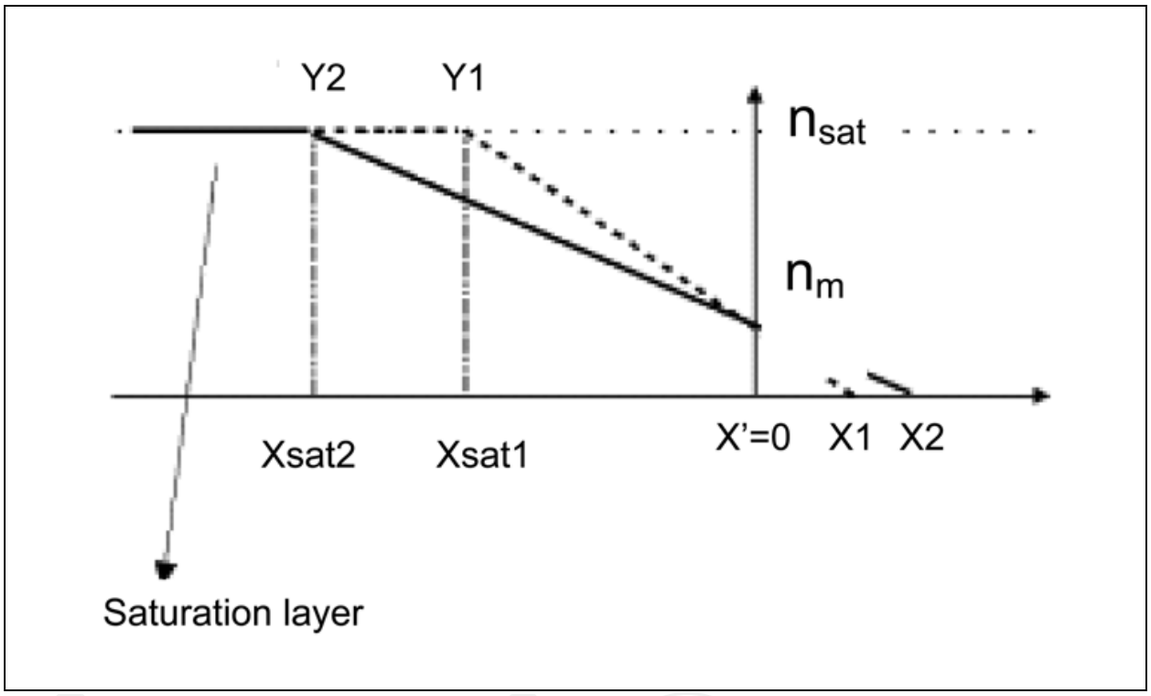

Fig. 6. Representation of the walkers distribution in the case Φ =1. Definition of the positions X_i and Y_i. x′(0) refers to the position where the concentration C_m is constant.

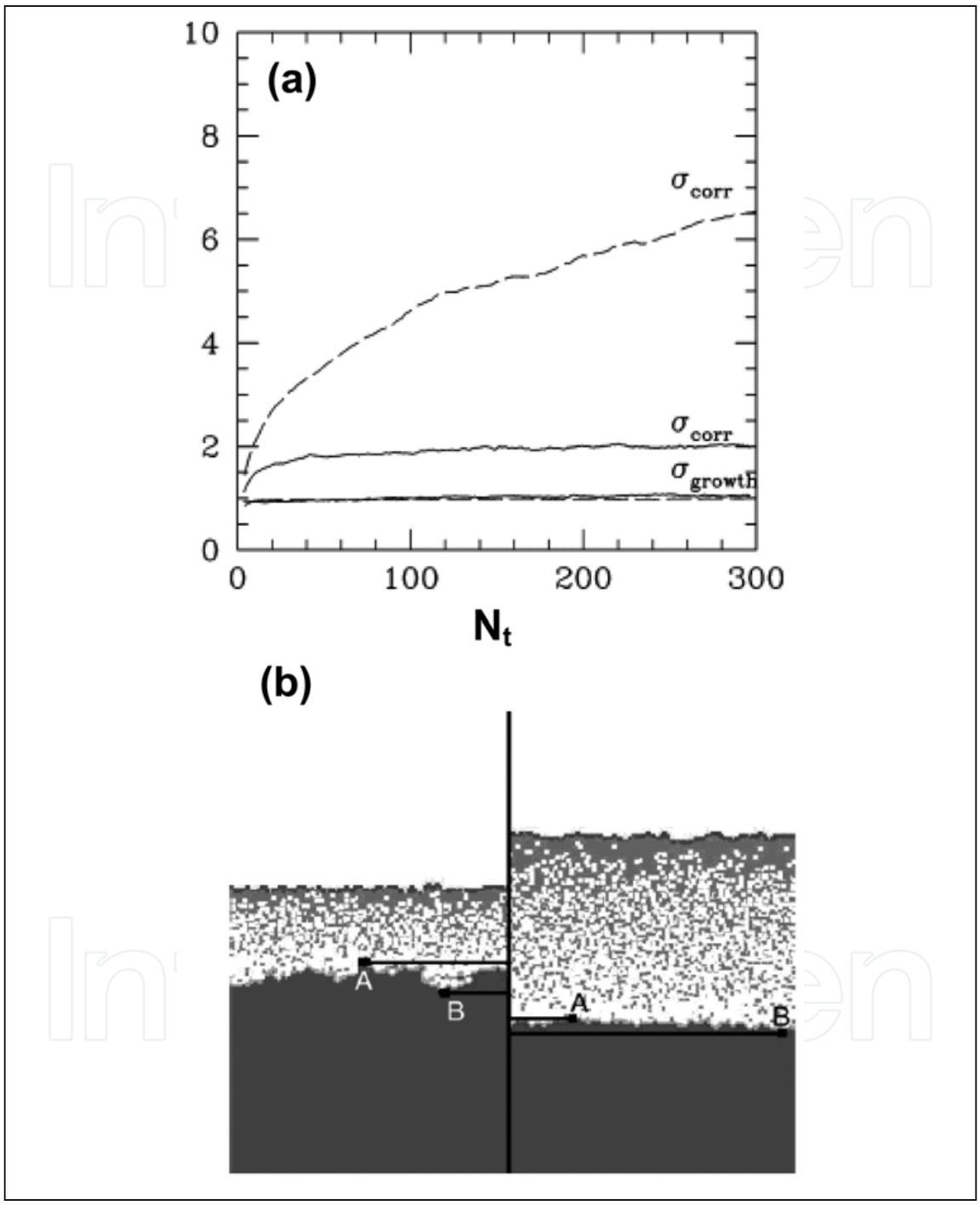

Fig. 7. Front roughness defined by (6) and (7). N_{corr}=10. (a) Φ =1 (dotted lines) and Φ =2 (solid lines) for the growth fronts (lower curves) and corrosion fronts (upper curves) as a function of the amount of material corroded Δh_{corr}. In figure 7(b) we can see the snapshot of the interface. Points A mark the uppermost and points B the lowermost positions of the corrosion front.

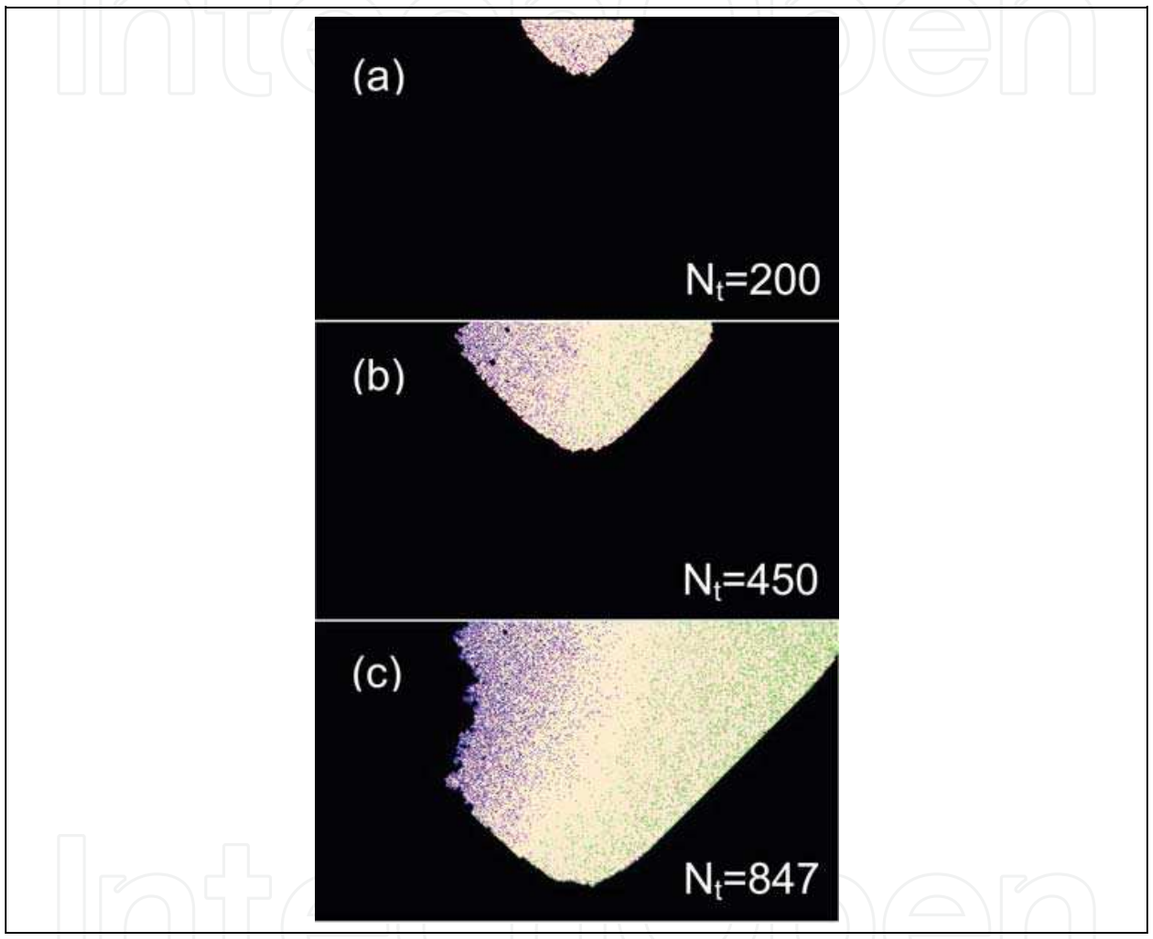

Fig. 8. Corresponding to the number of diffusion step N_{diff}=6000 and indicated simulation time steps (N_t). The green, blue and white colours correspond, respectively to acidic, basic and neutral zones.

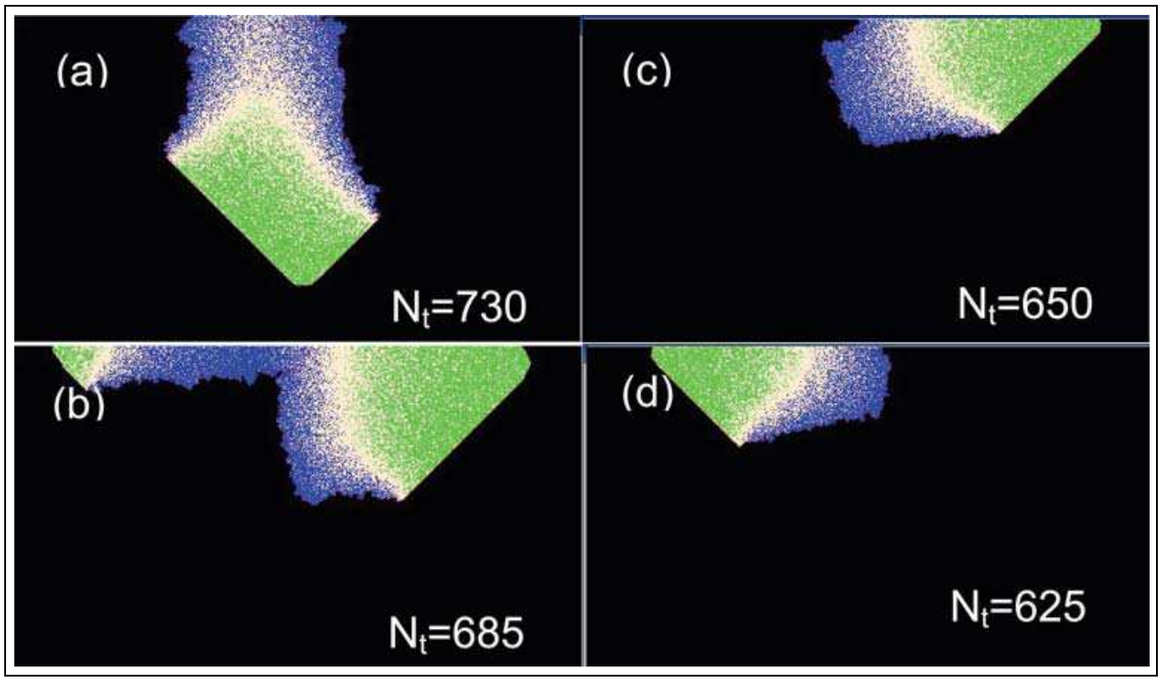

Fig. 9. Snapshots corresponding to the number of diffusion step N_{diff}=100 and indicated simulation time steps (N_t). The green, blue and white colours correspond respectively to acidic, basic and neutral zones.

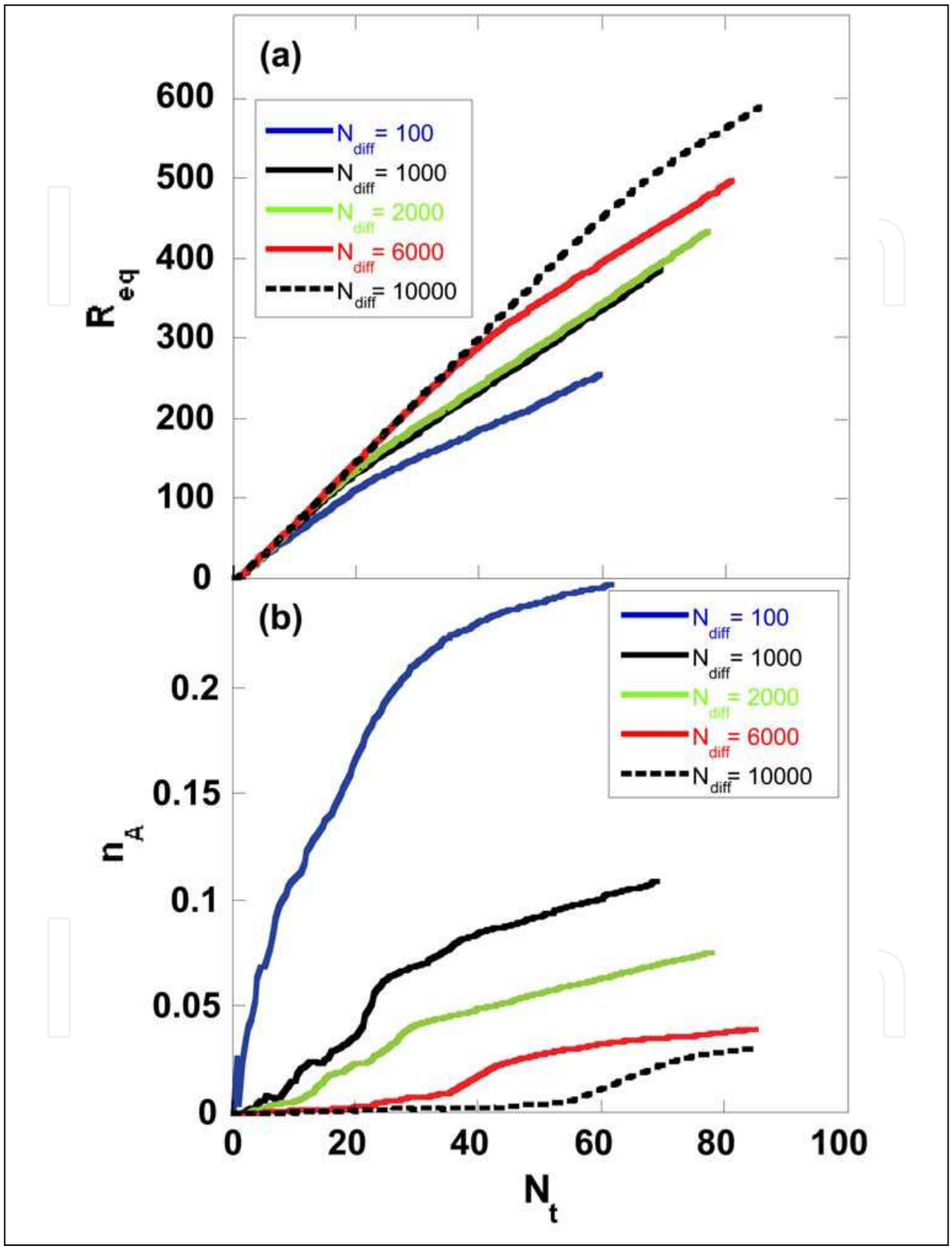

Fig. 10. (a)- Evolution of the equivalent radius (R_{eq}) versus the simulation time steps (N_t) for indicated number of diffusion step (N_{diff}). (b)- The evolution of the fraction of the acidic sites A (n_A) versus the simulation time steps, (N_t), for indicated number of diffusion step (N_{diff}).

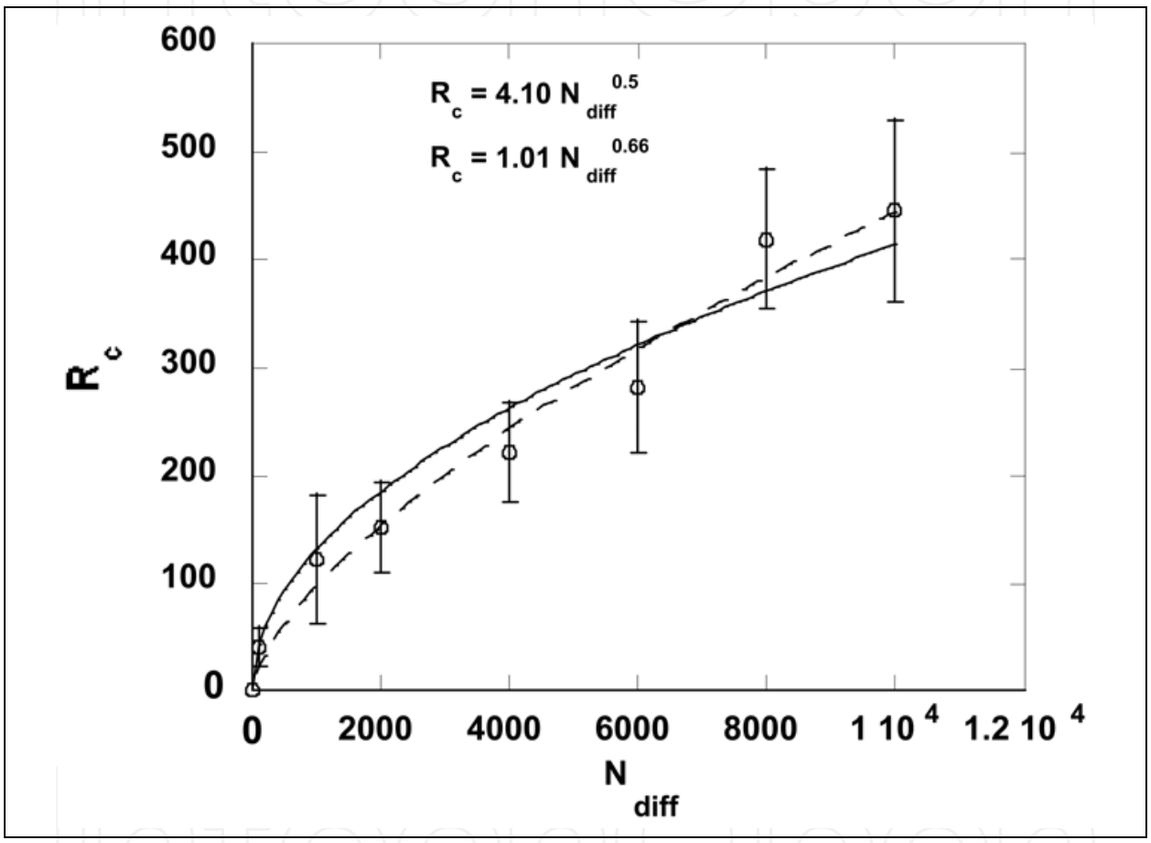

Fig. 11. Evolution of the critical radius (R_c), versus the diffusion step (N_{diff}). (_) the simulation data (o) the calculated result.

7. Equations

Equations are centred and numbered consecutively, from 1 upwards (Book Antiqua, 9pt).

$$E + R \rightarrow P \tag{1}$$

$$\langle h_{growth}(N_t)\rangle = \frac{1}{N_x}\sum_{i=1,N_x} h_{growth}(i) \tag{2}$$

$$\langle h_{corr}(N_t)\rangle = \frac{1}{N_x}\sum_{i=1,N_x} h_{corr}(i) \tag{3}$$

$$\langle h_{corr}(N_t)\rangle = h(0) - \frac{N_t N_{corr}}{N_x} \tag{4}$$

$$k(N_t) = \frac{d}{dN_t}\left[h(0) - \langle h_{corr}(N_t)\rangle\right] = \frac{d}{dN_t}\Delta h_{corr}(N_t) \tag{5}$$

$$\sigma_{growth}(N_t) = \left[\frac{1}{N_x}\sum_{i=1,N_x}\left(h_{growth}(i) - \langle h_{growth}(N_t)\rangle\right)^2\right]^{1/2} \tag{6}$$

$$\sigma_{corr}(N_t) = \left[\frac{1}{N_x}\sum_{i=1,N_x}\left(h_{corr}(i) - \langle h_{corr}(N_t)\rangle\right)^2\right]^{1/2} \tag{7}$$

$$E + (\Phi + 1)\, M \rightarrow P + (\Phi)\, D \tag{8}$$

$$\frac{n_m}{1} = \frac{X_i}{X_i + Y_i} \tag{9}$$

$$\frac{dY_i}{dX_i} = \frac{1 - n_m}{n_m} \tag{10}$$

$$(X_2 - X_1) + \frac{n_m}{2}X_2 - \frac{n_m}{2}X_1 \tag{11}$$

$$(Y_2 - Y_1)\frac{1 - n_m}{2}, \tag{12}$$

$$(Y_2 - Y_1)\frac{1 - n_m}{2} + (Y_2 - Y_1)(\phi - 1), \tag{13}$$

$$(Y_2 - Y_1)(1 + \frac{n_m}{2}) = (Y_2 - Y_1)[\frac{1 - n_m}{2} + (\phi - 1)]. \tag{14}$$

$$M + H_2O \rightarrow MOH_{aq} + e + H^+ \tag{15}$$

$$M + OH^- \rightarrow MOH_{solid} + e \tag{16}$$

$$H^+ + e \rightarrow \tfrac{1}{2} H_2 \quad (17)$$

$$H_2O + e \rightarrow \tfrac{1}{2} H_2 + OH^- \quad (18)$$

$$M + H_2O \rightarrow MOH_{aq} + \tfrac{1}{2} H_2 \quad (19)$$

$$M + H_2O \rightarrow MOH_{solid} + \tfrac{1}{2} H_2 \quad (20)$$

$$MOH_{solid} \rightarrow MOH_{aq} \quad (21)$$

$$H^+ + OH^- \rightarrow H_2O \quad (22)$$

$$R \rightarrow A, \quad N_{exc} \geq 0 \quad (23)$$

$$R+C(nn) \rightarrow P+E(nn), \quad N_{exc} < 0 \quad (24)$$

$$S+A(nn) \rightarrow S+E(nn), \quad N_{exc} \geq 0 \quad (25)$$

$$S+E(nn) \rightarrow S+C(nn), \quad N_{exc} < 0 \quad (26)$$

$$P \rightarrow E \quad (27)$$

$$A + C \rightarrow E + E \quad (28)$$

$$R_{eq} = \left(\frac{2N_{corroded}}{\pi}\right)^{1/2} \quad (29)$$

8. References

(Arrouvel et al., 2007) Arrouvel, C.; Diawara, B.; Costa, D. & Marcus, P. (2007). DFT periodic study of the adsorption of glycine on the anhydrous and hydroxylated (0001) surface of α Alumina J. Phys. Chem. C 111, 18164-1873.

(Balazs, 1996) Balazs, L. (1996). Corrosion front roughening in two dimensional pitting of aluminum thin layer. Phys Rev. E 54, 1183- 1189.

(Balazs & Gouyet, 1995) Balazs, L. & Gouyet, J. F. (1995). Two dimensional pitting corrosion of aluminium thin layer. Physica A 217, 319-338.

(Barabasi & Stanley, 1995) Barabasi, A. L. & Stanley, H. E. (1995). Fractal Concepts in Surface Growth, Cambridge University Press: Cambridge, NY.

(Bard & Foulkner, 1980) Bard, J. A. & Faulkner, L. B. (1980). Electrochemical Methods: Fundamentals and applications, John Wiley and Sons: NY.

(Cabrera & Mott, 1949) Cabrera, N & Mott, N. F. (1948). Theory of the oxidation of metals. Rep. Prog. Phys. 12, 163-184.

(Chopard & Droz, 1998) Chopard, B. & Droz, M. (1998). Cellular Automat Modelling of Physical Systems Cambridge University Press, NY.

(Cordoba-Torres et al 2001) Cordoba-Torres, P. ; Nogueira, R. P. ; De Miranda, L. ; Brenig, L. ; Wallenborn, J. & Fairen, V. (2001). Cellular automata simulation of asimple corrosion mechanism: mesoscopic heterogeneity versus macroscopic homogeneity. Electrochem. Acta 46, 2975-2989.

(De Gennes, 1991) De Gennes P. G. (1991). Scaling concepts in polymer physics Ed. Cornell University Press, NY.

(Eden, 1961) Eden, M. (1961). Proceeding of fourth Berkeley Symposium on Mathematical Stastics and Probability of California Press 1, Berkeley.

(Ernst & Newman, 2002) Ernst, P. & Newman, R. C. (2002). Pit growth studies instainless steel foils I. Introduction and pit growth kinetics. Corros. Sci. 44, 927-941.

(Glansdorff & Prigigine, 1971) Glansdorff, P. & Prigogine, I. (1971). (Eds), Structure Stabilité et Fluctuation Masson et Cie, Paris.

(Haseeb et al., 2001) Haseeb, A. S. M. A.; Schilardi, P. L.; Boltzan, A. E.; Piatti, R. C. V.; Salvarezza, R. R. & Arvia, A. J. (2001). Anodisation of copper in thiourea containing acid solution: part II in situ transversal imaging observations kinetics of anodic film growth. J. Electroanal. Chem. 500, 543-553.

(Kortlük, 1998) Kortlük, O. (1998). A general cellular automaton model for surface reactions. J. Phys. A: Math. Gren. 31, 9185-9189.

(Le Bellac, 1988) Le Bellac, M.; Barton, G. (1988) Quantum and Statistical Field Theory, Portland, OR: Booknew.

(Malki & Baroux, 2005) Malki, M. & Baroux, B. (2005). Computer simulation of corrosion pit growth. Corrs. Sci. 47, 171-182.

(Nicolis & Nicolis, 2001) Nicolis, C.; Kozak, J. J. & Nicolis, G. (2001). Encounter controlled reactions between intercating wlkers in finite lattices complex kinetics and many body effects. J. Chem. Phys. 115, 663-671.

(Nishida & Baba, 1996) Nishidate, K. & Baba, M. (1996). Cellular automaton model random walkers. Phys. Rev. Lett. 77, 1675-1678.

(Reigada et al., 1994) Reigada, R.; Sagués, F. & Costa, J. M. (1994). A Monte carlo simulation of localized corrosion. J. Chem. Phys. 101, 2329-2337.

(Saunier et al., 2005) Saunier, J. ; Dymitrowska, M. ; Chaussé, A. ; Stafiej, J. & Badiali, J. P. (2005). J. Electroanal. chem. 582, 267-273.

(Stafiej et al., 2006) Stafiej, J.; Taleb, A.; Vautrin-Ul, C.; Chausse, A. & Badiali, J. P. (2006). Passivation of Metals and Semiconductors, and Properties of Thin Oxide Layers, P. Marcus, V. Maurice (Eds), Elsevier, paris, pp 667-673.

(Taleb et al., 2001) Taleb, A.; Stafiej, J.; Chausse, A.; Messina, R. & Badiali, J. P. (2001). Simulation of film growth and diffusion during the corrosion process. J. Electroanal. Chem. 500, 554-561.

(Taleb et al., 2004) Taleb, A.; Chausse, A.; Dymitrowska, M.; Stafiej, J. & Badiali, J. P. (2004). Simulation of corrosion and passivation phenomena: Diffusion feedback on the corrosion rate. J. Phys. Chem. B, 108, 952-958.

(Taleb et al., 2007) Taleb, A. Stafiej, & J. Badiali, J. P. (2007). Numerical simulation of crystallographic corrosion : Particle production and surface roughness. Phys Chem. C 11, 9086-9094.

(Vautrin et al., 2007) Vautrin-Ul, C.; Taleb, A.; Chaussé, A.; Stafiej, J. & Badiali, J. P. (2007). Mesoscopic modelling of corrosion phenomena : Coupling between electrochemical and mechanical processes, analysis of the deviation from the faraday law. Electriochemica Acta 52, 5368-5376.

(Vautrin et al., 2008) Vautrin-Ul, C. ; Mendy, H. ; Taleb, A. ; Chaussé, A. ; Stafiej, J. & Badiali, J. P. (2008). Numerical simulation of spatial heterogeneity formation in metal corrosion. Corros. Sci. 50, 2149-2158.

(Vazquez et al., 1995) Vazquez, L.; Vara, J. M.; Herrasti, P.; Ocon, P.; Savarezza, R. C. & Arvia, A. J. (1995). Methods of fractal analysis applied to STM imaging. Chaos, Solitons and Fractales 6, 569-573.

Cellular Automata - Innovative Modelling for Science and Engineering

Edited by Dr. Alejandro Salcido

ISBN 978-953-307-172-5
Hard cover, 426 pages
Publisher InTech
Published online 11, April, 2011
Published in print edition April, 2011

Modelling and simulation are disciplines of major importance for science and engineering. There is no science without models, and simulation has nowadays become a very useful tool, sometimes unavoidable, for development of both science and engineering. The main attractive feature of cellular automata is that, in spite of their conceptual simplicity which allows an easiness of implementation for computer simulation, as a detailed and complete mathematical analysis in principle, they are able to exhibit a wide variety of amazingly complex behaviour. This feature of cellular automata has attracted the researchers' attention from a wide variety of divergent fields of the exact disciplines of science and engineering, but also of the social sciences, and sometimes beyond. The collective complex behaviour of numerous systems, which emerge from the interaction of a multitude of simple individuals, is being conveniently modelled and simulated with cellular automata for very different purposes. In this book, a number of innovative applications of cellular automata models in the fields of Quantum Computing, Materials Science, Cryptography and Coding, and Robotics and Image Processing are presented.

InTech Europe
University Campus STeP Ri
Slavka Krautzeka 83/A
51000 Rijeka, Croatia
Phone: +385 (51) 770 447
Fax: +385 (51) 686 166
www.intechopen.com

InTech China
Unit 405, Office Block, Hotel Equatorial Shanghai
No.65, Yan An Road (West), Shanghai, 200040, China
中国上海市延安西路65号上海国际贵都大饭店办公楼405单元
Phone: +86-21-62489820
Fax: +86-21-62489821

IntechOpen